pubs.acs.org/acschemicalbiology

Article

Beyond KRAS(G12C): Biochemical and Computational Characterization of Sotorasib and Adagrasib Binding Specificity and the Critical Role of H95 and Y96

Randa Mahran,[#] Jonas N. Kapp,[#] Salla Valtonen, Allison Champagne, Jinying Ning, William Gillette, Andrew G. Stephen, Feng Hao, Andreas Plückthun, Harri Härmä, Tatu Pantsar,[*] and Kari Kopra[*]

Cite This: https://doi.org/10.1021/acschembio.4c00315

Read Online

ABSTRACT: Mutated KRAS proteins are frequently expressed in some of the most lethal human cancers and thus have been a target of intensive drug discovery efforts for decades. Lately, KRAS-(G12C) switch-II pocket (SII−P)-targeting covalent small molecule inhibitors have finally reached clinical practice. Sotorasib (AMG-510) was the first FDA-approved covalent inhibitor to treat KRAS(G12C)-positive nonsmall cell lung cancer (NSCLC), followed soon by adagrasib (MRTX849). Both drugs target the GDP-bound state of KRAS(G12C), exploiting the strong nucleophilicity of acquired cysteine. Here, we evaluate the similarities and differences between sotorasib and adagrasib in their RAS SII−P binding by applying biochemical, cellular, and computational methods. Exact knowledge of SII−P engagement can enable targeting this site by reversible inhibitors for KRAS mutants beyond G12C. We show that adagrasib is strictly KRAS- but not KRAS(G12C)-specific due to its strong and unreplaceable interaction with H95. Unlike adagrasib, sotorasib is less dependent on H95 for its binding, making it a RAS isoform-agnostic compound, having a similar functionality also with NRAS and HRAS G12C mutants. Our results emphasize the accessibility of SII−P beyond oncogenic G12C and aid in understanding the molecular mechanism behind the clinically observed drug resistance, associated especially with secondary mutations on KRAS H95 and Y96.

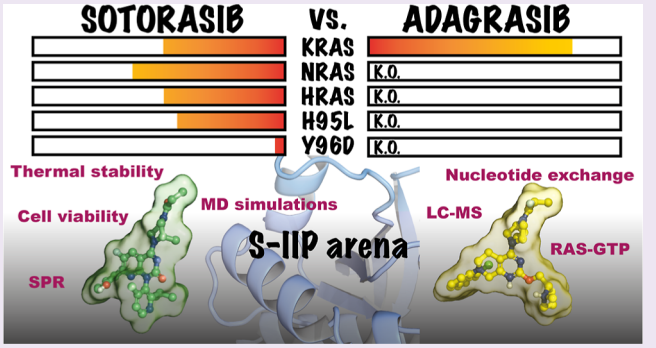

INTRODUCTION

RAS is frequently mutated in cancer, and RAS oncogenes have been reported in almost 30% of all malignant tumors.[1] Mutated RAS isoforms (KRAS/NRAS/HRAS) are most commonly found in solid tumors, including pancreatic, colorectal, and lung adenocarcinomas, as well as melanoma, making RAS a highly attractive target for a novel anticancer drug.[2−5] Oncogenic mutations promote RAS to occur mainly in the GTP-bound active state, due to diminished intrinsic GTPase activity, insensitivity to GTPase activating protein (GAPs), and/or elevated nucleotide exchange.[6,7] These changes are associated with tumorigenesis as a result of the constantly active RAS signaling pathways, promoting uncontrolled cell division and epithelial invasion. More than 85% of HRAS and 95% of both KRAS and NRAS mutations occur at the so-called "hotspot" codons, G12, G13, and Q61.[8] In the case of nonsmall cell lung cancer (NSCLC), KRAS(G12C) is found in ∼40% of all cases.[9] RAS was found to be a difficult drug target, and before the success with the covalent G12C inhibitors, it was even considered "undruggable".[1,10−13]

Covalent inhibitors offer prolonged target engagement, an advantage they have already demonstrated in clinical trials, also in the context of KRAS(G12C).[14−16] Two covalent KRAS-(G12C) inhibitors engaging the cryptic switch-II pocket (SII−P),[17,18] sotorasib (AMG-510; Lumakras/Lumykras), and adagrasib (MRTX849; KRAZATI) have recently been approved by FDA and EMA for the treatment of nonsmall cell lung cancer (NSCLC). Both inhibitors target the GDP-bound state of KRAS(G12C), trapping the protein in this inactive state and thus inhibiting the overactive KRAS downstream signaling. Successful targeting of KRAS(G12C) with this type of compounds does relies not only on the unique cysteine, which enables the covalent bond formation, but also on the intrinsic GTPase activity of KRAS(G12C).[19−21] The SII−P is more easily accessible and/or sampled more frequently when KRAS is GDP-bound, and this feature promotes targeting KRAS(G12C). However, at the same time, it can be considered rather unsuitable for some other

Received: May 6, 2024
Revised: September 6, 2024
Accepted: September 9, 2024

https://doi.org/10.1021/acschembio.4c00315
ACS Chem. Biol. XXXX, XXX, XXX−XXX

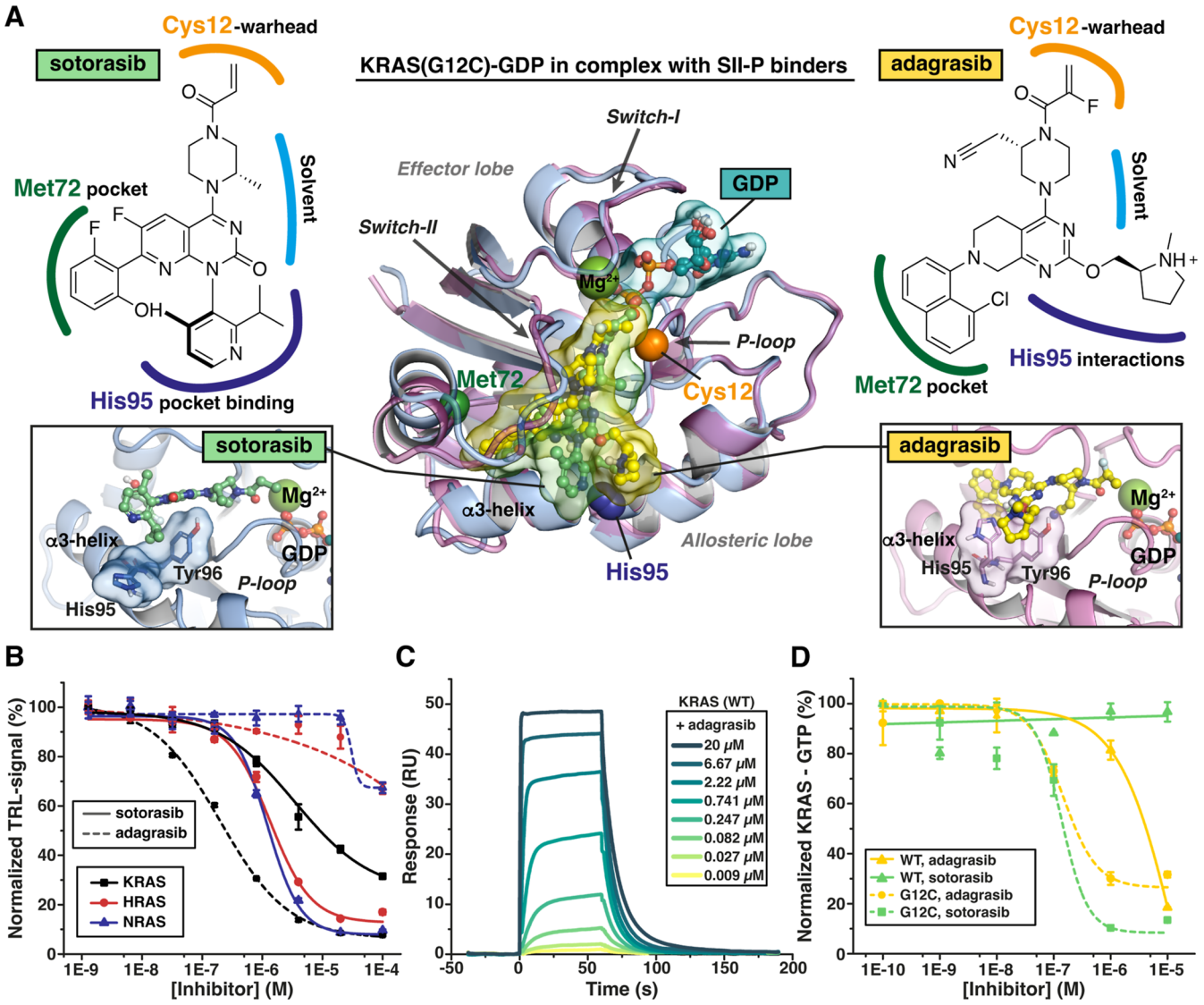

Figure 1. Adagrasib is KRAS-specific, while sotorasib binds equally to NRAS and HRAS. (A) Structures of sotorasib and adagrasib and their binding modes in KRAS switch-II pocket (SII−P). Superimposed KRAS(G12C) cocrystal structures are shown in the middle (PDB IDs: 6OIM and 6UT0[57,58]). A key-difference in their binding mode appears on KRAS-specific α3-helix residue H95, which is in out-conformation with sotorasib and in in-conformation with adagrasib (zoom-in illustrations). Sotorasib is depicted in a green ball and stick model, with the protein highlighted in blue cartoon; adagrasib is shown in a yellow ball and stick model, with protein highlighted in purple cartoon. The illustration includes GDP in a ball and stick model with teal carbons, and a Mg^{2+}-ion is shown as a green sphere; Cα-atoms of C12, M67, and H95 as orange, yellow, and blue spheres, respectively. (B) Concentration-dependent inhibition of SOS^{cat}-mediated guanine nucleotide exchange of 100 nM RAS after 30 min preincubation with sotorasib and adagrasib at RT (mean ± SD, n = 3). (C) Adagrasib SPR sensorgram showing concentration-dependent binding to KRAS(WT) (mean ± SD, n = 3). (D) G-LISA assay of GTP-bound RAS (see Materials and Methods) using starved cells incubated with adagrasib and sotorasib, followed by mitogenic stimulation and monitoring of RAS-GTP levels of the KRAS(WT) and KRAS(G12C) (mean ± SD, n = 3).

oncogenic KRAS alleles (e.g., G12R and Q61R) that are almost exclusively GTP-bound in cells.[22] Most recently, covalent targeting of the KRAS SII−P was demonstrated viable also for its GTP-bound state for the KRAS(G12C) and G12D.[23,24]

Even though there has been multiple attempts to use protein-derived or peptide-based RAS inhibitors using various epitopes, the cryptic SII−P has lately captured the spotlight.[25−29] SII−P has been extensively probed due to its dynamic nature, originating from the highly flexible switch-II region.[30] Many peptides and small molecule ligands have been designed to exploit this cryptic pocket for binding to RAS.[26−29,31−34] Early covalent inhibitors such as ARS-1620 targeted this pocket, however, with significantly compromised binding properties in comparison to the clinically approved sotorasib and adagrasib.[35,36] Both inhibitors have demonstrated clinical efficacy as monotherapy and are currently being evaluated in combination with other treatment modalities. Recently, resistance and reactivation of the RAS pathways after inhibitor treatment have been reported to occur via both on-target and off-target mechanisms.[36−46] The on-target mechanisms include alterations in the KRAS(G12C) SII−P composition. While clinical and preclinical data emerge, detailed information on the (noncovalent) binding specificities and interactions of these compounds toward other RAS proteins is unfortunately rather incomplete. Only recently,

https://doi.org/10.1021/acschembio.4c00315
ACS Chem. Biol. XXXX, XXX, XXX−XXX

Table 1. Sotorasib and Adagrasib Induced Effect on Different RAS Forms Using Four Different Assays

RAS	Inhibitor	Nucleotide exchange (IC_{50}, nM)	Thermal stability (ΔT_m, °C)	Cell GTP-RAS (IC_{50}, nM)	Cell viability (IC_{50}, nM)
KRAS(G12C)	Sotorasib	20.2 ± 1.9	26.4	137 ± 68	55.7 ± 5.3
	Adagrasib	4.3 ± 0.6	17.4	145 ± 12	7.6 ± 0.6
KRAS(WT)	Sotorasib	3500 ± 800	10.4[a]	> 10 μM	> 10 μM
	Adagrasib	200 ± 20	6.6[a]	2700 ± 300[b]	1000 ± 100[b]
KRAS(G12D)	Sotorasib	4300 ± 300	NM[c]	NM	NM
	Adagrasib	4700 ± 500	NM	NM	NM
KRAS(G12V)	Sotorasib	8200 ± 600	13.2[a]	NM	NM
	Adagrasib	3300 ± 600	1.9[a]	NM	NM
KRAS(G13D)	Sotorasib	6400 ± 500	10.2[a]	NM	NM
	Adagrasib	401 ± 89	6.6[a]	NM	NM
KRAS(Q61L)	Sotorasib	8000 ± 1200	3.9[a]	NM	NM
	Adagrasib	432 ± 52	4.7[a]	NM	NM
KRAS(H95L)	Sotorasib	> 10 μM	11.8[a]	NM	NM
	Adagrasib	> 10 μM	< 1.0	NM	NM
KRAS(Y96D)	Sotorasib	3400 ± 400	9.6[a]	NM	NM
	Adagrasib	> 10 μM	< 1.0	NM	NM
KRAS(G12C/H95L)	Sotorasib	167 ± 37	14.4[a]	122 ± 23	73.3 ± 6.9[d]
	Adagrasib	934 ± 80	4.1[a]	> 5 μM	4400 ± 900[b,d]
KRAS(G12C/Y96D)	Sotorasib	1600 ± 100	7.7[a]	NM	> 10 μM
	Adagrasib	> 10 μM	< 1.0	NM	1900 ± 200[b]
KRAS(G12C/R68M)	Sotorasib	NM	NM	NM	1100 ± 100
	Adagrasib	NM	NM	NM	94.2 ± 29.9
KRAS(G12C/Q99L)	Sotorasib	NM	NM	NM	75.8 ± 1.0
	Adagrasib	NM	NM	NM	175 ± 13
HRAS(WT)	Sotorasib	1300 ± 200	4.4[a]	> 5 μM	> 10 μM
	Adagrasib	> 10 μM	< 1.0	> 5 μM	1500 ± 400[b]
HRAS(G12C)[e]	Sotorasib	15.6 ± 5.6	NM	NM	53.0 ± 6.4
	Adagrasib	1300 ± 90	NM	NM	576 ± 51[b]
HRAS(G12D)[e]	Sotorasib	8500 ± 1000	NM	NM	NM
	Adagrasib	> 10 μM	NM	NM	NM
HRAS(G13D)[e]	Sotorasib	6900 ± 1000	NM	NM	NM
	Adagrasib	> 10 μM	NM	NM	NM
HRAS(Q61L)[e]	Sotorasib	> 10 μM	NM	NM	NM
	Adagrasib	> 10 μM	NM	NM	NM
NRAS(WT)	Sotorasib	1200 ± 200	10.2[a]	> 5 μM	3500 ± 1800
	Adagrasib	> 10 μM	< 1.0	> 5 μM	760 ± 29[b]
NRAS(G12C)[e]	Sotorasib	7.6 ± 1.3	NM	58.0 ± 6.7	17.4 ± 1.9
	Adagrasib	1300 ± 60	NM	840 ± 372[b]	1000 ± 100[b]

IC_{50} <0.1 0.1-0.5 0.5-2.5 μM ΔT_m >15°C

[a]No full stabilization with 100 μM inhibitor. [b]Values potentially relates to off-target toxicity. [c]NM not measured. [d]Assay performed with KRAS(G12C/H95Q). [e]RAS construct 1−169 aa.

SII−P engagement by noncovalent ligands has been systematically studied for the first time using sotorasib and adagrasib as model compounds.[18] In this context, Shokat et al. highlighted the accessibility of the SII−P for noncovalent ligands in various KRAS mutants beyond G12C.[18] Among the noncovalent inhibitors, MRTX1133, which targets G12D mutations, has already entered clinical trials.[46−48]

In this study, we elucidate the detailed binding mechanism of sotorasib and adagrasib as well as the mechanism by which resistance arises through mutations at residues H95 and Y96. Using an ultrasensitive thermal stability assay (TSA)[49−51] and nucleotide exchange assays[52−55] with HRAS, NRAS, and multiple KRAS mutants including H95L and Y96D mutations, we demonstrate distinct specificity profiles for sotorasib and adagrasib. Cell-based assays and molecular dynamics (MD) simulations support these biochemical results, providing atomic-level insights into the noncovalent binding specificities of these inhibitors. Both the biochemical and computational data reveal the irreplaceable nature of H95 and Y96 for interactions with sotorasib and adagrasib. Additionally, the results suggest a previously unidentified resistance mechanism of Y96D. Furthermore, we demonstrate potential mechanisms for direct target engagement of non-G12C oncogenic KRAS mutants via SII−P and for achieving KRAS specificity over NRAS and HRAS by exploiting interactions at residue H95. The data also reveal that, while adagrasib is KRAS-specific, sotorasib can effectively target not only KRAS(G12C) but also equally the G12C mutants of NRAS and HRAS. This potential offers new treatment possibilities for cancer patients harboring these rarer genetic alterations in NRAS and HRAS, even sotorasib is a less favorable starting point for noncovalent NRAS and HRAS mutant inhibition as adagrasib is for KRAS.

RESULTS AND DISCUSSION

Adagrasib Interacts Specifically with KRAS, While Sotorasib Targets All Forms of RAS(G12C) Equally. Sotorasib and adagrasib are clinically validated KRAS(G12C) inhibitors occupying the same SII−P, and both rely on covalent binding to Cys12 in an inactive, GDP-bound KRAS (Figure 1A).[20,56,57] To better understand the similarities and differences between these compounds, we measured the

https://doi.org/10.1021/acschembio.4c00315
ACS Chem. Biol. XXXX, XXX, XXX−XXX

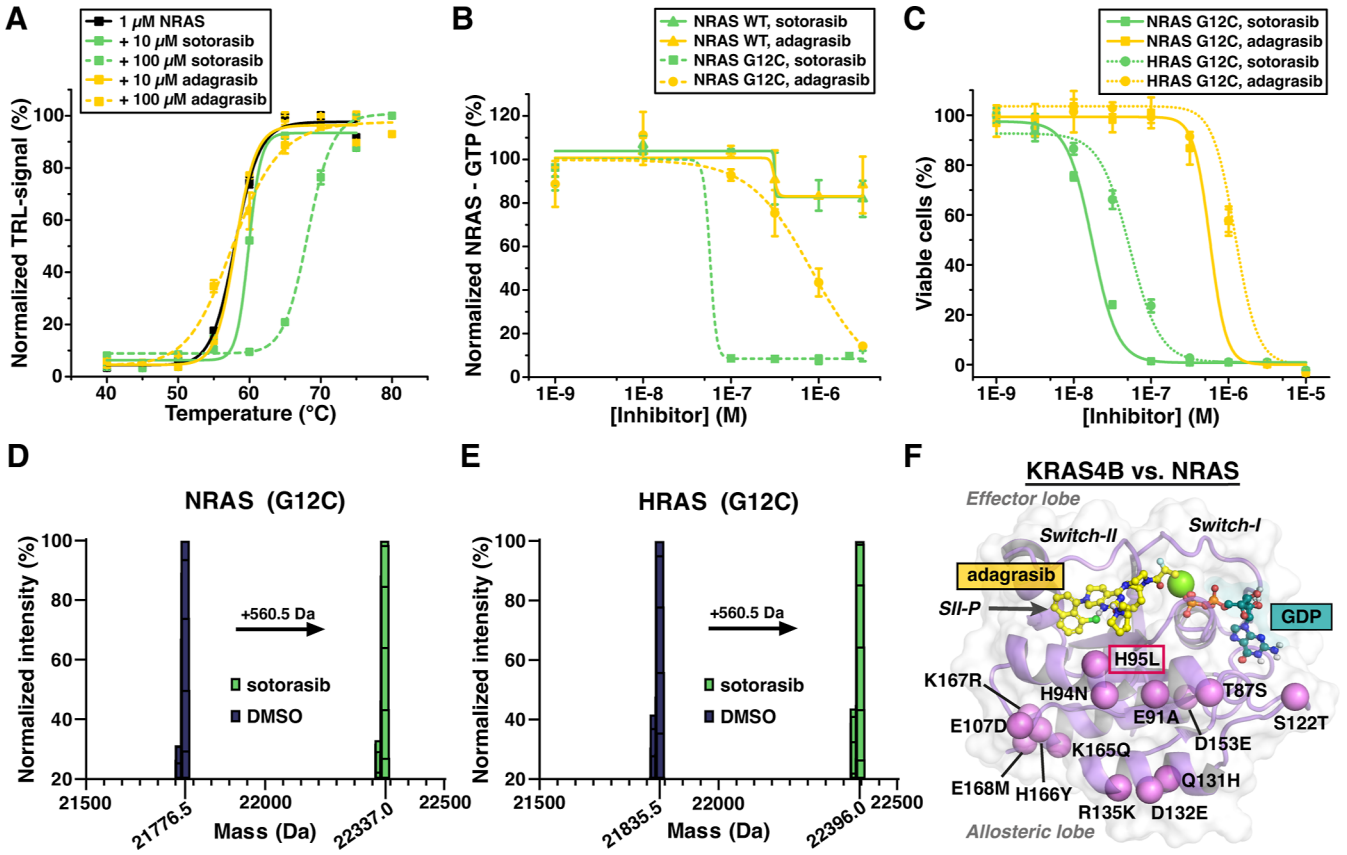

Figure 2. Sotorasib binds covalently to G12C mutants of KRAS, NRAS, and HRAS. (A) Concentration-dependent thermal stabilization of 1 μM NRAS after 30 min of preincubation with sotorasib and adagrasib at RT (mean ± SD, n = 3). (B) G-LISA assay of GTP-bound RAS using starved cells incubated with adagrasib and sotorasib, followed by mitogenic stimulation (10% FCS) and monitoring of RAS-GTP levels of the NRAS(WT) and NRAS(G12C) (mean ± SD, n = 3). (C) Cell viability assay with adagrasib and sotorasib using Ba/F3 cells stably expressing human NRAS and HRAS(G12C) (mean ± SD, n = 3). (D) Mass spectrometric analysis of sotorasib binding to NRAS(G12C) and (E) HRAS(G12C). (F) Structural differences between NRAS and KRAS. The only discrepancy in SII−P residues is observed at position 95.

binding of sotorasib and adagrasib to KRAS(G12C) and beyond with biochemical assays.[54,58−60] First, we used a nucleotide exchange assay to analyze the inhibitors' ability to lock RAS into its GDP-bound state and thereby block SOS^{cat}-mediated nucleotide exchange. With KRAS(G12C) used as a control, we found that IC_{50} values of both inhibitors were within the expected low nanomolar range (Figure S1A and Tables 1 and S2).[49,58,61] All nucleotide exchange results are listed in Table S2. Second, we used a TSA to analyze RAS thermal stability and inhibitor induced stability increase. The use of two independent external fluorescent probes, protein-probe (PP)[49−51] and 8-anilinonaphthalene-1-sulfonic acid (ANS), provided consistent results (Figure S1B). Both techniques show that sotorasib induces a slightly higher increase in KRAS(G12C) thermal stability compared with adagrasib (Table 1). In here, ANS was used as a secondary TSA assay, as in the used buffer conditions and protein concentration, data were compromised with SYPRO Orange, due to high stability of the protein−ligand complex and luminescence signal quenching.[49,62] All TSA results are listed in Table S3.

When analogous nucleotide exchange and TSA analyses were performed with KRAS(WT), adagrasib showed a clearer effect compared to sotorasib (Figures 1B, S2A, and S3). In nucleotide exchange assays with KRAS(WT), adagrasib exhibited IC_{50} values in the range of 200−300 nM as measured by quenching resonance energy transfer (QRET) and TR-FRET (Figures 1B and S3 and Tables 1 and S2). In contrast, sotorasib's effect was clearly diminished with KRAS(WT), with IC_{50} falling in the micromolar range (Figures 1B, S3, and Table 1). In TSA, both adagrasib and sotorasib stabilize KRAS(WT) only at very high concentrations (Table 1). At low micromolar concentrations, sotorasib especially displayed clear luminescence quenching in these assays, which could be partially compensated by the use of a higher RAS concentration in TSA with PP. However, as the ANS or SYPRO Orange could not be used as a control, we further confirmed these results using surface plasmon resonance (SPR) (Figures 1C and S4). SPR revealed a concentration-dependent response of adagrasib with KRAS(WT), while no response was seen with sotorasib (Figures 1C and S4). The observed k_{on} and k_{off} values were $1.11 \pm 0.05 \times 10^5$ and $9.24 \pm 0.77 \times 10^{-2}$ 1/s, giving a K_d of 0.78 ± 0.05 μM for binding of adagrasib to KRAS(WT). This value is in line with our nucleotide exchange assays observations, and previously reported SPR data showing that adagrasib is KRAS-specific and shows no binding to NRAS-(WT) or HRAS(WT).[63]

To verify the in vitro results in a cellular system, we measured the relative levels of active GTP-bound KRAS(WT) and KRAS(G12C) and performed cell viability assays with wild-type KRAS, HRAS, and NRAS (Figures 1D and S5). RAS-GTP levels were measured after the cells were starved in the presence of adagrasib and sotorasib followed by mitogenic stimulation with 10% fetal calf serum (FCS). This condition

https://doi.org/10.1021/acschembio.4c00315
ACS Chem. Biol. XXXX, XXX, XXX−XXX

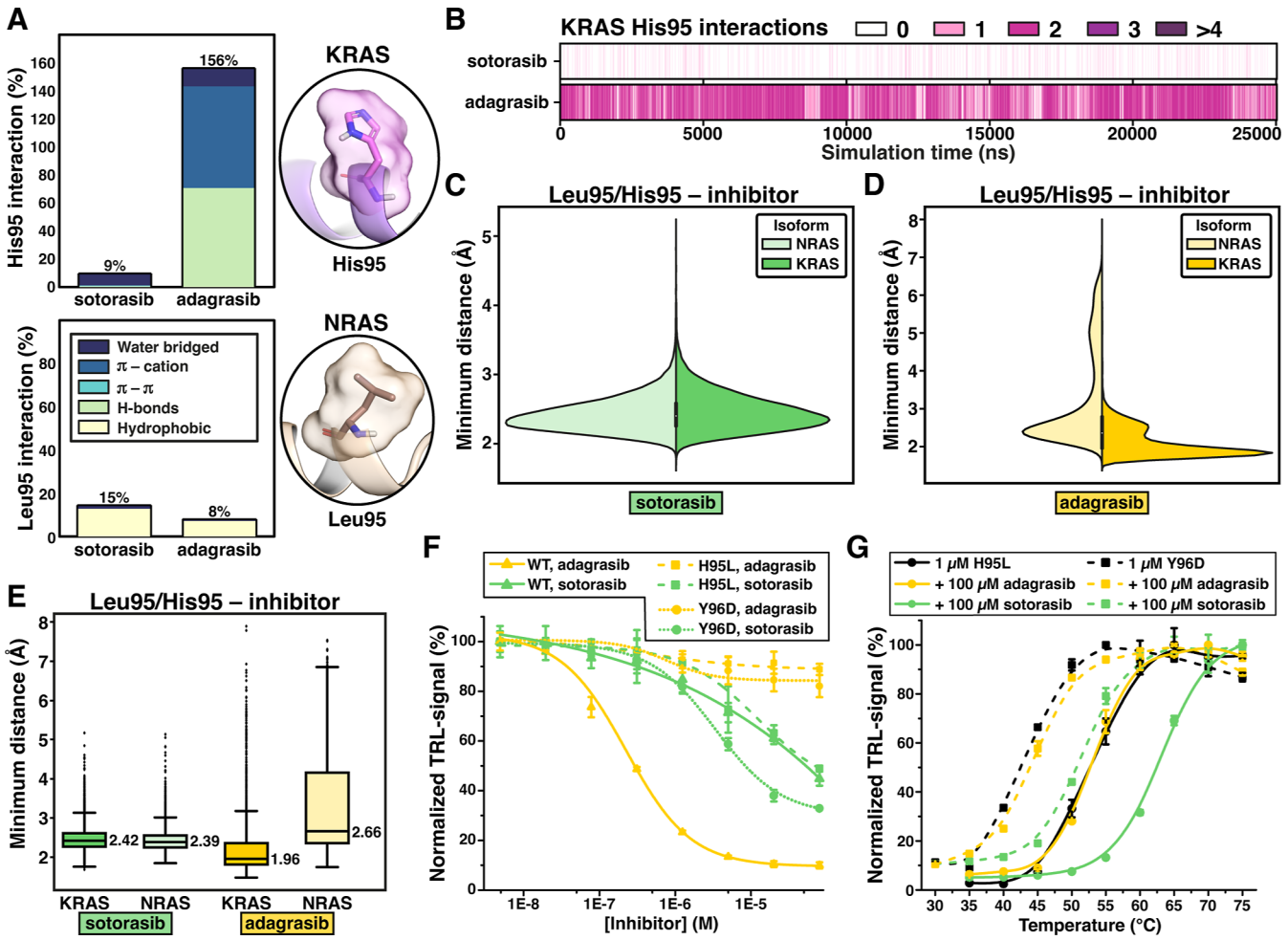

Figure 3. Adagrasib RAS isoform specificity is determined by His-95 of KRAS. (A) MD simulations show strong, high frequency interaction of adagrasib with His-95 (KRAS) but not with Leu-95 (NRAS). In contrast, sotorasib does not rely heavily on interactions with His-95 and even displays a slightly elevated interaction frequency with Leu-95. Interaction (%) related to the overall simulation time. Multiple simultaneous interactions may add up to over 100% interaction frequency. (B) KRAS His-95 interactions in the MD simulations with sotorasib and adagrasib are consistent throughout the simulations, as demonstrated by the observed interactions in time-specific plot of the concatenated trajectories (five individual 5 μs simulations). (C) Isoform-specific minimum distance of sotorasib to position 95 shown with violin plot. (D) Isoform-specific minimum distance of adagrasib to position 95 shown with violin plot. (E) Data of (C,D) are shown here with boxplots, with their median values. The black horizontal line in the box represents the median, and the box displays the quartiles of the data set (25−75%) and whiskers the rest of the data with maximum 1.5 interquartile range (IQR). Outliers are indicated with black diamonds. Data shown in (A−E) of each system (25 μs) were analyzed by each ns. (F) Concentration-dependent inhibition of SOS^{cat}-mediated guanine nucleotide exchange of 100 nM KRAS(WT), KRAS(H95L), and KRAS (Y96D) after 30 min preincubation with sotorasib and adagrasib at RT (mean ± SD, n = 3). (G) Concentration-dependent thermal stabilization of 1 μM KRAS(H95L) and KRAS (Y96D) after 30 min preincubation with sotorasib and adagrasib at RT (mean ± SD, n = 3).

was selected to mimic the nucleotide exchange assays *in cellulo*. Both adagrasib and sotorasib demonstrated comparable inhibition of KRAS(G12C) activation at the expected concentrations (Table 1).[57,58,61] Next, we confirmed the cross-reactivity of adagrasib on KRAS(WT) at micromolar concentrations (>1 μM), while sotorasib did not show any effect at the tested concentrations (Figure 1D). On the other hand, adagrasib started to exhibit KRAS-independent toxicity already at low micromolar concentrations (Figure S5). Toxicity was also observed in the cell viability assays using Ba/F3 cells stably expressing human KRAS(G12C) or wild-type KRAS, NRAS, and HRAS. Adagrasib induced toxicity has also been reported earlier, and it is like to be as a result from off-target effect, potentially through inhibition of several kinases.[44,64] In KRAS(G12C) expressing cells, both compounds inhibited viability at low nanomolar concentrations (Table 1). In contrast, in the case of K/N/HRAS(WT) expressing cells, only a minor effect on cell viability was observed with sotorasib (Figure S5 and Table 1).

As the effect of sotorasib on the wild-type RAS isoforms was much weaker than that for adagrasib, we next tested if KRAS mutations at positions G12, G13, and Q61 would alter the accessibility of the SII-pocket for both inhibitors (Figure S6). In the QRET nucleotide exchange assay, KRAS mutations G13D and Q61L had no significant effect on adagrasib inhibitory activity over KRAS(WT), while G12D and G12 V mutations increased the IC_{50} value approximately 10-fold in comparison to that of KRAS(WT) (Table 1). This was confirmed by the TSA, in which adagrasib stabilization was more pronounced with KRAS(G13D) and KRAS(Q61L), compared with KRAS(G12 V) (Figure S7). The weak effect of sotorasib on nucleotide exchange observed for KRAS(WT)

https://doi.org/10.1021/acschembio.4c00315
ACS Chem. Biol. XXXX, XXX, XXX−XXX

was similar to that of all four tested KRAS mutants, indicating low affinity against all non-G12C KRAS proteins (Figure S6 and Table 1). However, at a high sotorasib concentration (100 μM), a clear stabilization for KRAS(G12 V), KRAS(Q61L), and KRAS(G13D) was monitored (Figure S7).

Adagrasib showed no binding to HRAS(WT) or NRAS-(WT) in the QRET nucleotide exchange assays (IC_{50} > 10 μM) (Figure 1B). Sotorasib, in contrast, displayed IC_{50} values of 1.2−1.3 μM for HRAS(WT) and NRAS(WT), indicating weak binding (Figure 1B). Furthermore, TR-FRET nucleotide exchange and cell viability assays indicate that the effect of sotorasib might be stronger on NRAS(WT) compared to that on KRAS(WT) (Figures S3 and S5). We could further observe stabilization of NRAS(WT) by sotorasib but not with adagrasib (Figures 2A and S2). Together, these data suggest that sotorasib might have comparable efficacy against NRAS-(G12C) and HRAS(G12C) mutants as against KRAS(G12C), which is in line with the very recent clinical findings.[65]

To assess the potential relevance of targeting cancers harboring NRAS(G12C) and/or HRAS(G12C) mutants, we explored the Catalogue of Somatic Mutations in Cancer (COSMIC v99) (Figure S8).[66] In the case of KRAS, G12C mutations account for 11.6% (5519 and 47,503) of all missense mutations. G12C mutations are found less frequently for NRAS and HRAS in the database, representing 2.7% (240/8835) and 1.6% (43/2614) of all NRAS and HRAS missense mutations, respectively (Figure S8). While the number of patients with non-KRAS(G12C) mutations is relatively small, our analysis confirms their existence. These patients may potentially benefit from treatment with sotorasib. Further investigation is warranted to determine whether these mutations can be considered as disease-relevant drivers.[65]

To further demonstrate the isoform-agnostic binding behavior of sotorasib, we performed a panel of assays to explore its binding specificity. Cellular RAS-GTP assays confirmed that sotorasib targets NRAS(G12C) and KRAS-(G12C) to a similar extent, while adagrasib inhibition is KRAS-specific (Figures 1D and2B). Cell viability assays further confirmed that HRAS(G12C) can be targeted by sotorasib as well (Figure 2C). In the QRET nucleotide exchange assay with NRAS(G12C) and HRAS(G12C), low nanomolar range inhibition was observed with sotorasib, as the IC_{50} value with adagrasib was reduced over 300-fold in comparison to KRAS(G12C) (Figure S9 and Tables 1 and S2). We additionally confirmed the covalent attachment of sotorasib to NRAS(G12C) and HRAS(G12C) by a liquid chromatography-mass spectrometry (LC-MS) assay (Figure S10). The highest peak (12.2 min) from the separation was analyzed by MS (Figure S10), and in the case of both NRAS(G12C) (Figure 2D) and HRAS(G12C) (Figure 2E), 560.5 Da increase in molecular weight (MW) was observed in the presence of sotorasib (calculated MW 560.59 Da) (Figures 2 and S11). Strikingly, the only residue that differs between the three RAS isoforms within the SII−P is found in position 95, which is His, Leu, or Gln in the case of KRAS, NRAS, and HRAS, respectively (Figures 2F and S12).

His-95 Residue of KRAS Confers Isoform Specificity of Adagrasib. To rationalize our findings related to the WT isoform binding and specificity of the two inhibitors (Table 1), we conducted MD simulations with noncovalently bound adagrasib and sotorasib in SII−P with KRAS(WT) and NRAS(WT) (Figure S13). These simulations suggest that the observed key-interactions are mainly isoform-agnostic for sotorasib, while this is not the case for adagrasib (Figures S14 and S15). The most significant discrepancy between the inhibitors is observed for interactions with position 95 (Figures 3A−E, S14, and S15). Adagrasib displays a high interaction frequency with KRAS His-95 (Figure 3A). It displays multiple simultaneous interactions to this residue, namely, H-bond to N of the pyrimidine ring and cation−π interaction to methylpyrrolidine, which adds up to over 100% interaction frequency (156%). Interactions toward the residue in this position are dramatically diminished (8%) when the residue is leucine, as found in NRAS (Figures 3A and S12). In contrast, sotorasib's interaction frequency with position 95 is slightly elevated with Leu-95 (15%) in comparison to His-95 (9%). Sotorasib introduces the pyridyl ring with an isopropyl substituent next to these residues. The observed interactions of both inhibitors with KRAS His-95 and NRAS Leu-95 are consistent throughout the simulations (Figures 3B and S16). Moreover, adagrasib, which exhibits a tighter contact to His-95 than sotorasib, displays clear instability when it is in complex with NRAS and in the region where Leu-95 is present, which is demonstrated by the increased distance to this residue (Figure 3C−E). Sotorasib maintains a consistent distance to the residue at position 95, regardless of the RAS isoform (Figure 3C,E). Overall, our simulation results suggest that the interactions of adagrasib with H95 are deterministic for its KRAS(WT) binding and selectivity over those of other RAS(WT) isoforms. In contrast, sotorasib's interactions with H95 are not essential, allowing for higher tolerance for amino acid variations in this position.

In addition to the irreplaceable role of KRAS H95 for adagrasib, our MD simulations showed close contacts and high interaction frequency of both inhibitors with Tyr-96 (Figure S17), an additional secondary mutation site that has been reported to confer resistance in the clinic.[17,35,38] To validate the individual importance of KRAS H95 and Y96, we created two single mutant constructs; KRAS(H95L) reflecting the native SII−P present in NRAS(WT) and KRAS(Y96D) linked to the acquired resistance with G12C targeting inhibitors.[38] During the characterization of these mutants without an inhibitor, we found KRAS(Y96D) to have a negative impact on SOS^{cat} induced nucleotide exchange (Figure S18). Even more importantly, KRAS(Y96D), but not KRAS(H95L), showed significantly reduced thermal stability in comparison to KRAS(WT) (Figures S18 and S19 and Table S3), also confirmed by SYPRO Orange. When the nucleotide exchange assay was performed with inhibitors, we observed a reduced inhibition with sotorasib using KRAS(H95L) compared with KRAS(WT) (Figure 3F and Table 1 and S2). In the case of adagrasib, however, both mutants were resistant to nucleotide exchange inhibition, indicating nonexisting binding at the tested concentrations. Thermal stability results of sotorasib with KRAS(H95L) and KRAS(Y96D) are highly similar to those monitored with KRAS(WT), while adagrasib exhibited negligible stabilization with both mutants (Figures 3G and S2 and Table S3).

KRAS(G12C) Secondary Mutations at His-95 and Tyr-96 Disrupt Sotorasib and Adagrasib Binding. In order to obtain more biologically relevant data, we created two double mutants, KRAS(G12C/H95L) and KRAS(G12C/Y96D). Characterization of these mutants revealed that KRAS-(G12C/H95L) exhibited slightly faster SOS^{cat}-induced nucleotide exchange than KRAS(G12C), and the nucleotide exchange activity of KRAS(G12C/Y96D) was rescued

https://doi.org/10.1021/acschembio.4c00315
ACS Chem. Biol. XXXX, XXX, XXX−XXX

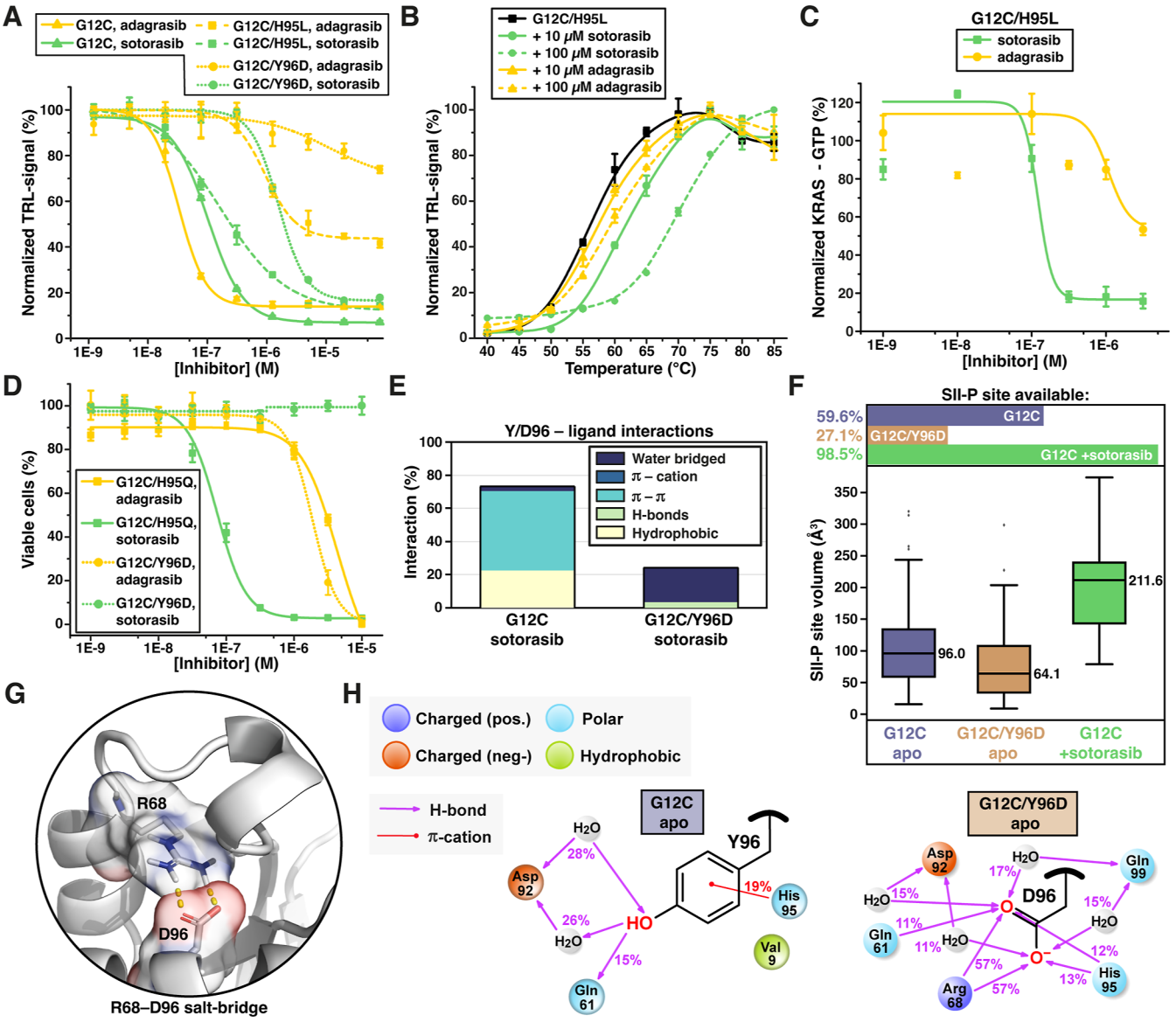

Figure 4. Adagrasib function is compromised by KRAS(G12C) secondary mutations at positions H95 and Y96. (A) Concentration-dependent inhibition of SOS^{cat}-mediated guanine nucleotide exchange of 100 nM KRAS(G12C), KRAS(G12C/H95L), and KRAS(G12C/Y96D) after 30 min preincubation with sotorasib and adagrasib at RT (mean ± SD, n = 3). (B) Concentration-dependent thermal stabilization of 1 μM KRAS(G12C/H95L) after 30 min preincubation with sotorasib and adagrasib at RT (mean ± SD, n = 3). (C) G-LISA assay of GTP-bound RAS using starved cells incubated with adagrasib and sotorasib, followed by mitogenic stimulation (10% FCS) and monitoring of RAS-GTP levels of the KRAS(G12C/H95L) (mean ± SD, n = 3). (D) Cell viability assay with adagrasib and sotorasib using Ba/F3 cells stably expressing human KRAS(G12C/H95Q) and (G12C/Y96D) (mean ± SD, n = 3). (E) Observed Y96 and Y96D interactions of noncovalently bound sotorasib in MD simulations of KRAS(G12C) and KRAS(G12C/Y96D) systems. (F) Observed SII−P availability and volume in GDP-bound apo simulations of KRAS(G12C) and KRAS(G12C/Y96D), and with KRAS(G12C) with noncovalently bound sotorasib. Pocket availability and size (when available) for the 20 μs simulation data of each system was analyzed for each 50 ns with SiteMap. Boxplots consist of 239, 109, and 395 (of 401) data points for KRAS(G12C) apo, KRAS(G12C/Y96D) apo, and KRAS(G12C) + sotorasib simulations, respectively. (G) Putative interaction between D96 and R68. A representative snapshot of a G12C/Y96D apo SII−P simulation displaying the potential interaction. (H) Observed interactions of the position 96 side chains Y96 and D96 in the simulations without the SII−P ligand. Interactions with >10% frequency are shown. Data consist of 20 μs simulations for each system.

compared to KRAS(Y96D) (Figure S18A). KRAS(G12C/H95L) and KRAS(G12C/Y96D) showed increased thermal stability over their single mutant forms, even though KRAS(G12C/Y96D) stability was still reduced in comparison to that of KRAS(G12C) (Figures S18B and S19 and Table S3).

The effect of these double mutations was also evident in a nucleotide exchange assay with both sotorasib and adagrasib. Here, we could observe inhibition for KRAS(G12C/H95L) and KRAS(G12C/Y96D) with sotorasib but with compromised affinity in comparison to KRAS(G12C) (Figure 4A and Table 1). Adagrasib showed negligible inhibition with KRAS(G12C/Y96D), but surprisingly retained some low-level functionality with KRAS(G12C/H95L) (Figure 4A and Table 1). Using KRAS(G12C/H95L), thermal stability increased with the addition of 10 μM sotorasib, while adagrasib only modestly increased the stability of this mutant (Figure 4B and Table 1). With KRAS(G12C/Y96D), only 100 μM

https://doi.org/10.1021/acschembio.4c00315
ACS Chem. Biol. XXXX, XXX, XXX−XXX

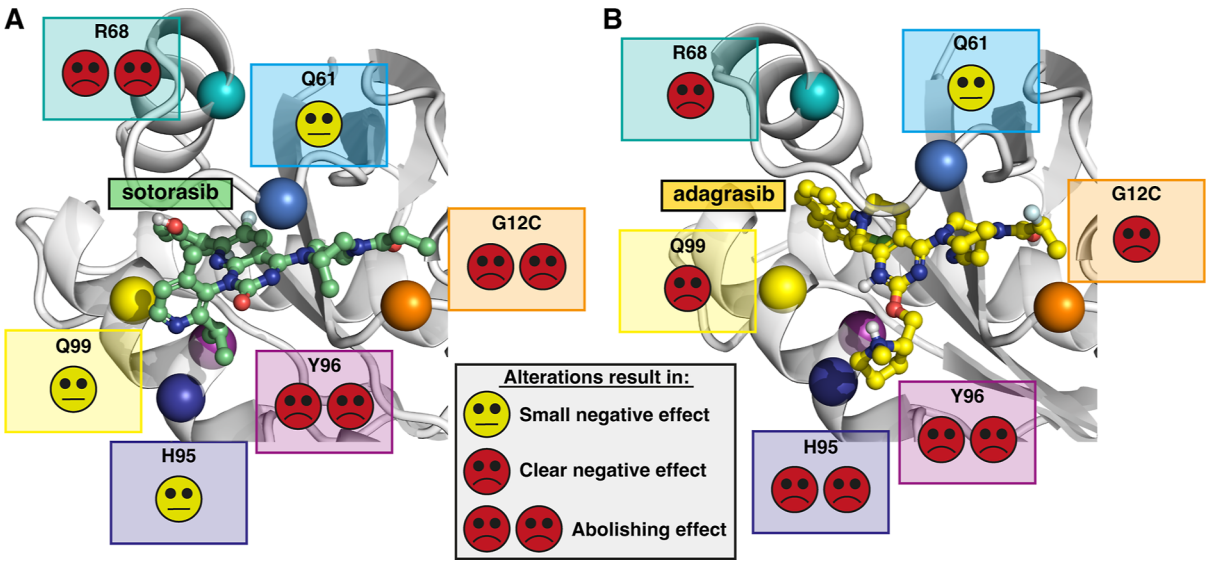

Figure 5. Summary of the impact of the tested SII−P alterations on sotorasib and adagrasib interaction. (A) In addition to G12C, sotorasib binding is highly dependent on R68 and Y96. Mutations at positions Q99 and Q61 have small negative effect on its binding, and H95 mutations are quite well tolerated. (B) Adagrasib binding relies heavily on H95, and it is also nontolerant to Y96 mutations. Adagrasib is more tolerant to R68 alterations and slightly less tolerant to Q99 mutations in comparison to sotorasib. Additionally, it binds readily to KRAS(WT).

sotorasib yielded a measurable increase in the thermal stability (Figure S19). Although the nucleotide exchange and thermal stability results with KRAS(G12C/H95L) are not directly aligned, kinetic nucleotide exchange experiments indicate that sotorasib binds covalently to KRAS(G12C/H95L) (Figure S21). Most likely, the weakened binding of adagrasib as a result of the H95L mutation is overrepresented in the thermal shift assay in comparison to results obtained in the nucleotide exchange assay (Figures 3G and4B).

In our cell-based RAS-GTP assay, we could indeed confirm that the inhibitory effect of sotorasib is not compromised by the H95 mutation in comparison to KRAS(G12C), while the inhibition by adagrasib is nearly abolished (Figures 1D and 4C and Table 1). Cell viability results with either KRAS(G12C/H95Q), the HRAS derived mutant, or KRAS(G12C/Y96D) are consistent with the previous findings (Figure 4D). We observed that the IC_{50} values for sotorasib were comparable when applied to the double mutants KRAS(G12C/H95Q) and KRAS(G12C), while the effect of the inhibitor on KRAS-(G12C/Y96D) was negligible. Adagrasib, on the other hand, followed the non-RAS-driven decrease in cell viability and did not show a specific response in cell viability for cells expressing either KRAS(G12C/H95Q) or KRAS(G12C/Y96D) (Figures 4D and S5B and Table 1).

To provide more insights into the role of the secondary mutation Y96D and its negative impact on SII−P inhibitor binding, we conducted MD simulations of the KRAS mutants G12C and G12C/Y96D with noncovalently bound sotorasib in SII−P. These simulations provide insights into the stability of the inhibitor in the binding site before the covalent reaction takes place with C12. Similarly, as observed in KRAS(WT) simulations, Tyr96 frequently interacts with sotorasib in the context of the G12C mutation, including $\pi-\pi$ and hydrophobic interactions (Figures 4E and S22). These key-interactions are abolished by the Y96D mutation, which consequently leads to the instability of sotorasib in the binding site (Figures 4E, S22, and S23). In fact, complete dissociation of sotorasib from the switch-II pocket was observed at 2000 ns of the simulation in one of the five simulation replicas (Figure S23).

Furthermore, we conducted additional simulations of both GDP-bound KRAS(G12C) and G12C/Y96D SII−P apo structures to observe if the mutation itself has any impact on the binding pocket (Figures 4F−H and S24). The resistance-mediating double mutation G12C/Y96D appears to constrict SII−P compared to G12C (Figure 4F). This is highlighted by the reduced availability of the SII−P (expressed as the % of the frames where it is found) and its decreased volume (expressed as median volumes). The pocket with a median volume of 64.1 $Å^3$ is only available in 27.1% of the analyzed frames according to SiteMap, compared to 96.0 $Å^3$ and 59.6% in the context of KRAS(G12C). Remarkably, with sotorasib bound in the SII−P of KRAS(G12C), the pocket volume median is increased by a factor of 2 to a median volume of 211.6 $Å^3$, confirming the dynamic and inducible nature of this pocket. A detailed view on the simulation results allows us to identify a putative molecular mechanism of the inaccessibility of the SII−P. The mutated Y96D appears to promote a novel intraprotein interaction, a salt-bridge between D96 and R68; thereby influencing the size and accessibility of the pocket (Figure 4G,H). In addition, this suggests a competitive mechanism where the D96-R68 interaction may preclude the inhibitor's own interaction with R68. With sotorasib, this interaction was indeed compromised in simulations with G12C and Y96D (Figure S22). The negative effect of the Y96D mutation on nucleotide exchange might also be connected to the interaction of SOS E1002 in its "active" conformation (Figure S25). Consequently, the de novo salt-bridge between D96 and R68 may reduce the KRAS−SOS interaction.[67,68]

In a next step, we evaluated the effect of mutations of the residues R68 and Q99 in a cell viability assay (Figure S26).[37,40,44] Q99 is located close to the SII−P in the α3-helix (Figure S27) and has been shown to confer resistance to adagrasib while not affecting the clinical activity of sotorasib.[44,56] We could indeed confirm this with an ∼20-fold shift in the potency of adagrasib in the context of

https://doi.org/10.1021/acschembio.4c00315
ACS Chem. Biol. XXXX, XXX, XXX−XXX

KRAS(G12C/Q99L)-expressing cells (Figure S26 and Table 1). In addition, our MD simulations with KRAS(WT) show mainly water-mediated interactions of both inhibitors with Q99 (Figure S27). As the Q99L mutation only affects adagrasib binding,[44] this mutation may distort the neighboring H95 (in) conformation, which is critical for adagrasib, thus having an indirect effect on adagrasib binding (Figure S27). Clinically reported mutations at the R68 residue in KRAS-(G12C) include R68S and R68M.[37] The R68S mutation blocks drug binding of both adagrasib and sotorasib, leading to resistance to these inhibitors.[37] In contrast, R68 M has been reported to confer resistance to sotorasib but remains sensitive to adagrasib. Again, we could confirm the clinical observation by demonstrating that sotorasib's effect on cell viability was drastically reduced in cells expressing KRAS(G12C/R68M), while adagrasib's effect remained unchanged (Figure S26). These results are in line with our simulation observations, where only sotorasib displays direct interactions with R68 with high frequency (Figure S15). We speculate that while the integrity of the SII−P is retained by the similar-sized methionine mutation (R68M), the shorter serine (R68S) might be detrimental to the pockets' integrity. The R68S mutation likely leads to a compromised shielding of the hydrophobic SII−P from solvent exposure, affecting the pocket interactions with both inhibitors (Figure S28).[37] Further research is needed to disclose whether these R68 mutations could have an impact on nucleotide exchange via affecting an important interaction with SOS (Figure S25).

Although both inhibitors occupy the same SII−P, sotorasib and adagrasib display different interaction profiles, and their tolerance for mutations varies considerably (Figure 5 and Tables 1, S2, and S3). This has to be taken into an account when new and improved drugs are developed and when selecting the correct drug for individual patient. Adagrasib has already been shown to serve as a starting scaffold to target other KRAS mutations beyond G12C, including noncovalent inhibitors such as MRTX1133 for KRAS(G12D) and KRAS-(G13D) targeting compounds.[48,69,70] These developed non-covalent inhibitors utilize H95 for their affinity and KRAS specificity and, instead of the warhead, salt bridge for mutation specificity. Sotorasib targets all RAS G12C mutants similarly. Thus, it can be speculated if it could serve as a starting point for noncovalent targeting of oncogenic NRAS or HRAS. In the case of NRAS and HRAS, G12 mutants are not the most relevant (Figure S8). NRAS possess most often Q61 mutations, while HRAS mutations are more equally spread to all the three RAS hotspot positions.[71,72] Many of these NRAS and HRAS mutations are not easily targeted in their GDP-form as in the cellular context, the active GTP-form is highly overrepresented due to their negligible intrinsic GTPase activity and/or fast nucleotide exchange rates.[71,72] However, as shown with KRAS, in most cases, the highly limited cycling can be enough for targeting these RAS mutants using RAS-GDP targeting compounds.[73] Thus, we tested if sotorasib behaves similarly to KRAS with hotspot HRAS and NRAS mutants in addition to G12C (Figure S29). Thermal stability assays with NRAS(Q61R), and HRAS mutants (Q61L, G13D, and G12D) indicates that mutations cause similar type of changes in RAS behavior than in the case of KRAS, as Q61R has the highest stabilizing and G13D highest destabilizing effect (Figure S29A and Table S3).[49] These stability changes are linked especially to intrinsic nucleotide exchange activity, and lack of measurable NRAS(Q61R) intrinsic or SOS^{cat} induced nucleotide exchange, similar to KRAS(Q61R), was expected.[49,74] This lack of nucleotide cycling makes RAS(Q61R) mutants highly unlikely targets in their GDP-form. HRAS mutants (Q61L, G13D, and G12D) all gave clearly measurable stimulation in nucleotide exchange upon SOS^{cat} addition and were investigated with sotorasib and adagrasib in the QRET nucleotide exchange assay (Figure S29B). As expected, adagrasib showed no nucleotide exchange inhibition with these HRAS proteins, as sotorasib induced micromolar range inhibition as in the case of the same KRAS mutants (Figures S6 and S29B and Table S2). Sotorasib affinity to RAS(WT) and these hotspot mutants is rather weak, which increases the level of potential assay interferences. However, these assays clearly highlight the sotorasib behavior as an isoform-agnostic RAS inhibitor. This is quite the opposite to adagrasib, having rather high KRAS(WT) binding affinity but negligible interaction with either NRAS or HRAS (Figures S3 and S4 and Table S2). It remains to be seen if introducing additional modifications in the sotorasib scaffold (e.g., removal of the warhead) would offer an improved potential for pan-RAS inhibitory activity. Adagrasib and sotorasib share features with ARS-1620, but the development has been done in opposite directions. ARS-1620 forms a hydrogen bond to His95, showing clear KRAS(G12C) specificity over NRAS and HRAS G12C mutants (Figure S30).[33] Interactions to H95 are further enhanced with adagrasib, but in the case of sotorasib, the absence of strong interaction to this position is causing the RAS isoform-agnostic behavior. Potentially, by modifying the pyridyl ring in sotorasib to increase the interaction with L95 (NRAS) or Q95 (HRAS), RAS isoform selective inhibitors could be developed (Figure S12). To our knowledge, there are no published data on the activities of the similar scaffold containing compounds, such as garsorasib, glecirasib, and MK-1084, toward the other RAS isoforms.[75−77]

CONCLUSIONS

Sotorasib and adagrasib, the first FDA-approved drugs for KRAS, are both inhibitors that occupy the SII−P.[43,44,78] However, their specific interactions with the pocket residues result in individual specificity profiles. Unsurprisingly, this leads to previously reported secondary mutations, inducing drug resistance.[46] KRAS(Y96D) was one of the first reported secondary mutations for adagrasib resistance, and the same mutation was found to confer resistance to multiple KRAS-(G12C) inhibitors currently in clinical trials.[38] Later, other KRAS alterations outside the "hotspot" area, such as R68 and H95, have been reported.[37] H95 has been identified as an adagrasib-specific resistance mutation, as sotorasib better tolerates mutations in this position.[37]

We studied both sotorasib and adagrasib interactions in relation to these reported secondary mutations causing clinical resistance to find mechanisms causing the resistance and potentially how those could be avoided. Our data obtained both from biochemical and cell-based assays clearly indicate that adagrasib specificity is driven by its strong interaction with KRAS-specific H95, while sotorasib depends heavily on its interaction with Y96, which is conserved in all RAS isoforms. MD simulations further support these observations, additionally indicating that sotorasib is a pan-RAS(G12C) drug. Building on this observation, we could demonstrate covalent engagement of NRAS(G12C) and HRAS(G12C) to sotorasib. Additionally, its efficacy and unchanged pan-RAS(G12C) binding affinity were proven in biochemical assays and cell

https://doi.org/10.1021/acschembio.4c00315
ACS Chem. Biol. XXXX, XXX, XXX−XXX

lines expressing these mutants. We thereby show that sotorasib could be used for patients carrying a NRAS(G12C) or HRAS(G12C), consistent what was recently reported.[65] Rubinson et al. identified a patient with NRAS(G12C) colorectal cancer who was treated with the combination of sotorasib and the anti-EGFR antibody panitumumab. The patient achieved a marked tumor response with reduction in liver metastases, providing a clinical proof-of-concept that sotorasib can be effective in patients with NRAS(G12C) mutated tumors.[65] It was also shown that the sotorasib response to NRAS and HRAS hotspot mutants is similar to the ones in KRAS, further confirming the RAS isoform-agnostic behavior.

Finally, our MD simulations suggest that the Y96D mutation may confer resistance to the majority of SII−P binders by reducing pocket availability via minimizing pocket volume through a de novo salt-bridge between D96 and R68. Mutations in the position R68, also as such, abolished sotorasib binding. Overall, the results presented here can support the ongoing development of KRAS or pan-RAS drugs beyond G12C, clearly highlighting the importance of the different SII−P amino acids. Our results also highlight how a panel of different methods can unravel functionalities and support each other, when inhibitors are studied in vitro, and also how these finding can be explained by molecular modeling and simulations.

MATERIALS AND METHODS

Protein Expression and Purification. Detailed lists of materials and instrumentation are provided in the Supporting Information Appendix. Details of production and purification of SOS^{cat} (564−1048), RAS(WT) proteins [HRAS (1−189), KRAS(2−188), and NRAS(1−189)], KRAS mutants (G12C, G12D, G12 V, G13D, and Q61L), and truncated NRAS(Q61R, 1−169), HRAS(G12D, 1−169), HRAS(G13D, 1−169), and HRAS(Q61L, 1−169) have been described previously.[49,52] Avi-KRAS(1−188) production and purification has also been described elsewhere, and full-length Avi-HRAS and Avi-NRAS were created accordingly.[49] Details on protein expression and purification of NRAS(G12C, 1−169), HRAS(G12C, 1−169), KRAS(H95L, 1−188), KRAS(Y96D, 1−188), KRAS-(G12C/H95L, 1−188), and KRAS(G12C/Y96D, 1−188) are provided in the Supporting Information Appendix with more details.

Nucleotide Exchange Assay. Nucleotide exchange assays were performed using QRET and time-resolved Förster resonance energy transfer (TR-FRET) in 384-well plate and methods were described previously.[53−55,79] Briefly, in the QRET assay, a soluble quencher (2.5−4.0 μM MT2) is used together with 2′/3′-position Eu^{3+}-chelate conjugated GDP or GTP (10−50 nM Eu^{3+}-GTP and Eu^{3+}-GDP).[53] RAS (10−100 nM) and SOS^{cat} (5−10 nM) were used in all QRET assays in a final volume of 15 μL. TR-FRET assays were performed using Avi-tagged RAS(WT) (10 nM) proteins and 5 nM of Eu^{3+}-chelate conjugated streptavidin (SA-Eu^{3+}) as a donor, and AF647-GTP (50 nM) as acceptor.[55] Nucleotide exchange was initiated with SOS^{cat} (5 or 10 nM) and performed in a 10 μL final volume. The full protocol is provided in the Supporting Information Appendix.

Thermal Stability Assays. All RAS thermal stability assays were performed in 96-well plates mainly by using a two-step protein-probe assay with 50 or 1000 nM RAS concentrations in 8 μL (heating) prior detection solution addition (65 μL).[49,51,62,80] Two DSF dyes (10 μM ANS and 5 × SYPRO Orange), used as a control, were employed with a one-step protocol and 10 μM RAS with or without 20 μM adagrasib and sotorasib in a final 20 μL volume.[49,51,60,62] The full protocol is provided in the Supporting Information Appendix.

RAS-GTP Assays. A cell culture protocol for RAS-GTP assays is provided in the Supporting Information Appendix. Quantification of RAS-GTP was performed using the absorbance-based G-LISA Ras Activation Kit (Cytoskeleton, BK131), where a coated RAS-binding domain only captures GTP-bound RAS. After cell lysis with the supplied buffer, the bound protein content was determined by the supplied protein assay. Depending on the transfected construct, 6−22 μg of whole-cell lysate was used in duplicate for the RAS-GTP assay. To ensure that only the transfected RAS isoform or mutant is detected, we replaced the supplied primary and secondary detection antibodies with a mouse anti-HA antibody (Sigma, H9658) and a goat antimouse HRP antibody (Pierce, 31,438).

Cell Viability Assays. Assays were performed using mouse Ba/F3 cell lines stably expressing exogenous KRAS(WT) or KRAS bearing the studied amino acid mutation (G12C, G12C/R68M, G12C/H95Q, G12C/Y96D, and G12C/Q99L) (KYinno biotechnology, Peking, China). Additionally, Ba/F3 cell lines stably expressing HRAS(WT) and HRAS(G12C) or NRAS(WT) and NRAS(G12C) were used. Cell culture and CellTiter-Glo assays using sotorasib and adagrasib were performed according to manufacturer's instructions (KYinno biotechnology and Promega). Briefly, cells were cultured in 10% FBS supplemented RPMI-1640 medium and seeded in 96-well plates (3000 cells/well). Cells were cultured overnight prior to the addition of sotorasib and adagrasib (0−10 μM) and plates were further incubated for 72 h. Cell viability was measured using a CellTiter-Glo assay according to the manufacturer's instruction by measuring the luminescence signal (Envision, PerkinElmer, Waltham, MA).

LC-MS Binding Studies. Recombinant NRAS(G12C, 1−169) and HRAS(G12C, 1−169) were incubated in an assay buffer [50 mM HEPES (pH 7.4), 2 mM TCEP, 125 mM NaCl, and 10 mM $MgCl_2$] with either 0.1% DMSO or 10 μM sotorasib in 0.1% final DMSO for 1 h at RT and subsequently submitted to the LC-MS service at the Functional Genomics Center Zurich. A detailed protocol is provided in the Supporting Information Appendix.

Molecular Dynamics Simulations. Molecular modeling was conducted with Maestro (Schrödinger release 2020−2, Schrödinger LLC, New York, NY) with OPLS3e force field,[81,82] using Desmond MD engine for the simulations.[83] More detailed description of the system preparation and simulations is provided in the Supporting Information Appendix. In brief, simulations with noncovalently bound sotorasib and adagrasib in SII−P were based on their published cocrystal structures (PDB ID: 6OIM[58] and 6UT0[57]). Engineered residues of the structures were reverse mutated to the native ones, and specific mutations were introduced to obtain the studied systems (Table S1). Protein preparation wizard[84] prepared systems were solvated in a 15 Å cubic box with TIP3P water with 150 mM K^+ and Cl^- salt (adjusted to a neutral net charge).[85] Prior to the production simulations, the default Desmond relaxation was applied for all of the systems. The production simulations (4−5 μs) were run in NpT ensemble (p = 1.01325 bar; T = 310 K) with settings as in previous report,[86] resulting generally in 20−25 μs aggregate of simulation data for each system (Table S1). The analysis of trajectories were conducted with Schrödinger Maestro tools. Analysis of SII−P volume was conducted with trajectory_binding_site_volumes.py script (Schrödinger LLC) by analyzing every 50th frame (50 ns intervals) of the trajectories using residues 12, 58, 72, and 96 for the site definition.

ASSOCIATED CONTENT

Data Availability Statement

Data generated during the study are available upon request. The original MD simulation Desmond raw trajectories, generated and analyzed in the study, have been deposited in the Zenodo repository and are freely available at: 10.5281/zenodo.10812233 and 10.5281/zenodo.10781452.

Supporting Information

The Supporting Information is available free of charge at https://pubs.acs.org/doi/10.1021/acschembio.4c00315.

Additional experimental details; materials; methods; and biological, biochemical, and computational data (PDF)

https://doi.org/10.1021/acschembio.4c00315
ACS Chem. Biol. XXXX, XXX, XXX−XXX

AUTHOR INFORMATION

Corresponding Authors

Tatu Pantsar − *School of Pharmacy, Faculty of Health Sciences, University of Eastern Finland, 70210 Kuopio, Finland;* orcid.org/0000-0002-0369-2909; Email: tatu.pantsar@uef.fi

Kari Kopra − *Department of Chemistry, University of Turku, 20500 Turku, Finland;* orcid.org/0000-0001-7585-6020; Email: kari.kopra@utu.fi

Authors

Randa Mahran − *Department of Chemistry, University of Turku, 20500 Turku, Finland*

Jonas N. Kapp − *Department of Biochemistry, University of Zurich, 8057 Zurich, Switzerland*

Salla Valtonen − *Department of Chemistry, University of Turku, 20500 Turku, Finland*

Allison Champagne − *NCI RAS Initiative, Frederick National Laboratory for Cancer Research, Frederick, Maryland 21702, United States*

Jinying Ning − *KYinno Biotechnology Co., Ltd., Beijing 101111, China*

William Gillette − *NCI RAS Initiative, Frederick National Laboratory for Cancer Research, Frederick, Maryland 21702, United States*

Andrew G. Stephen − *NCI RAS Initiative, Frederick National Laboratory for Cancer Research, Frederick, Maryland 21702, United States*

Feng Hao − *KYinno Biotechnology Co., Ltd., Beijing 101111, China*

Andreas Plückthun − *Department of Biochemistry, University of Zurich, 8057 Zurich, Switzerland;* orcid.org/0000-0003-4191-5306

Harri Härmä − *Department of Chemistry, University of Turku, 20500 Turku, Finland;* orcid.org/0000-0002-8936-039X

Complete contact information is available at: https://pubs.acs.org/10.1021/acschembio.4c00315

Author Contributions

#R.M. and J.N.K. contributed equally to this work. T.P. and K.K. designed research; R.M., J.K., S.V., A.C., J.N, T.P., and K.K. performed research; R.M., J.K., S.V., A.C., J.N, W.G., A.G.S., F.H., T.P., and K.K. analyzed data; and R.M., J.K., A.P., H.H., T.P., and K.K. wrote the paper.

Notes

The authors declare the following competing financial interest(s): Harri Hrm has commercial interest through QRET Technologies Ltd. Jinying Ning and Feng Hao have commercial interest through KYinno Biotechnology Co., Ltd.

ACKNOWLEDGMENTS

This work was supported by Academy of Finland (323433/K.K., 329012/K.K., and 353324/K.K.) and Krebsliga Schweiz grants (KFS-4147-02-2017 and KFS-5290-02-2021-R to A.P.). This project was funded in part with federal funds from the National Cancer Institute, National Institutes of Health Contract HHSN261200800001E. The content of this publication does not necessarily reflect the views or policies of the Department of Health and Human Services, and the mention of trade names, commercial products, or organizations does not imply endorsement by the US government. The authors would like to thank Matt Drew, Peter Frank, Phuong Vi Le, Randy Gapud, José Sánchez Hernández, Jennifer Mehalko, Shelley Perkins, Nitya Ramakrishnan, Mukul Sherekar, Kelly Snead, Simon Messing, Troy Taylor, Vanessa Wall, and Tim Waybright from the Frederick National Laboratory for Cancer Research, Frederick MD, USA for cloning, expression, purification, and QC of the used small GTPase proteins. The authors wish to acknowledge CSC−IT Center for Science, Finland, for computational resources. The authors gratefully acknowledge the Functional Genomics Center Zurich (FGCZ) of University of Zurich and ETH Zurich, and in particular Serge Chesnov, for the support on Proteomics analyses.

REFERENCES

(1) Moore, A. R.; Rosenberg, S. C.; McCormick, F.; Malek, S. RAS-targeted Therapies: is the Undruggable Drugged? *Nat. Rev. Drug Discovery* **2020**, *19* (8), 533−552.

(2) Raphael, B. J.; Hruban, R. H.; Aguirre, A. J.; Moffitt, R. A.; Yeh, J. J.; Stewart, C.; Robertson, A. G.; Cherniack, A. D.; Gupta, M.; Getz, G.; et al. Integrated Genomic Characterization of Pancreatic Ductal Adenocarcinoma. *Cancer Cell* **2017**, *32* (2), 185−203.e13.

(3) Muzny, D. M.; Bainbridge, M. N.; Chang, K.; The Cancer Genome Atlas Network; et al. Comprehensive Molecular Characterization of Human Colon and Rectal Cancer. *Nature* **2012**, *487* (7407), 330−337.

(4) Akbani, R.; Akdemir, K. C.; Aksoy, B. A.; Albert, M.; Ally, A.; Amin, S.; Arachchi, H.; Arora, A.; Auman, J.; Ayala, B.; et al. Genomic Classification of Cutaneous Melanoma. *Cell* **2015**, *161* (7), 1681−1696.

(5) Collisson, E. A.; Campbell, J. D.; Brooks, A. N.; The Cancer Genome Atlas Research Network; et al. Comprehensive Molecular Profiling of Lung Adenocarcinoma. *Nature* **2014**, *511* (7511), 543−550.

(6) Lu, S.; Jang, H.; Nussinov, R.; Zhang, J. The Structural Basis of Oncogenic Mutations G12, G13 and Q61 in Small GTPase K-Ras4B. *Sci. Rep.* **2016**, *6*, 21949.

(7) Kim, D.; Xue, J. Y.; Lito, P. Targeting KRAS(G12C): From Inhibitory Mechanism to Modulation of Antitumor Effects in Patients. *Cell* **2020**, *183* (4), 850−859.

(8) Murugan, A. K.; Grieco, M.; Tsuchida, N. RAS Mutations in Human Cancers: Roles in Precision Medicine. *Semin. Cancer Biol.* **2019**, *59*, 23−35.

(9) Dogan, S.; Shen, R.; Ang, D. C.; Johnson, M. L.; D'Angelo, S. P.; Paik, P. K.; Brzostowski, E. B.; Riely, G. J.; Kris, M. G.; Zakowski, M. F.; et al. Molecular Epidemiology of EGFR and KRAS Mutations in 3,026 Lung Adenocarcinomas: Higher Susceptibility of Women to Smoking-related KRAS-mutant Cancers. *Clin. Cancer Res.* **2012**, *18* (22), 6169−6177.

(10) Cox, A. D.; Fesik, S. W.; Kimmelman, A. C.; Luo, J.; Der, C. J. Drugging the Undruggable RAS: Mission Possible? *Nat. Rev. Drug Discov.* **2014**, *13* (11), 828−851.

(11) Khan, I.; Rhett, J. M.; O'Bryan, J. P. Therapeutic Targeting of RAS: New Hope for Drugging the "Undruggable. *Biochim. Biophys. Acta Mol. Cell Res.* **2020**, *1867* (2), 118570.

(12) Uprety, D.; Adjei, A. A. KRAS: From Undruggable to a Druggable Cancer Target. *Cancer Treat. Rev.* **2020**, *89*, 102070.

(13) Molina-Arcas, M.; Samani, A.; Downward, J. Drugging the Undruggable: Advances on RAS Targeting in Cancer. *Genes (Basel)* **2021**, *12* (6), 899.

(14) McCormick, F. Sticking it to KRAS: Covalent Inhibitors Enter the Clinic. *Cancer Cell* **2020**, *37* (1), 3−4.

(15) Li, H.; Qi, W.; Wang, Y.; Meng, L. Covalent Inhibitor Targets KRasG12C: A New Paradigm for Drugging the Undruggable and Challenges Ahead. *Genes Dis.* **2023**, *10* (2), 403−414.

(16) Boike, L.; Henning, N. J.; Nomura, D. K. Advances in Covalent Drug Discovery. *Nat. Rev. Drug Discovery* **2022**, *21* (12), 881−898.

(17) Pantsar, T. KRAS(G12C)−AMG 510 Interaction Dynamics Revealed by All-Atom Molecular Dynamics Simulations. *Sci. Rep.* **2020**, *10* (1), 11992.

(18) Vasta, J. D.; Peacock, D. M.; Zheng, Q.; Walker, J. A.; Zhang, Z.; Zimprich, C. A.; Thomas, M. R.; Beck, M. T.; Binkowski, B. F.; Corona, C. R.; et al. KRAS is Vulnerable to Reversible Switch-II Pocket Engagement in Cells. *Nat. Chem. Biol.* **2022**, *18* (6), 596−604.
(19) Nagasaka, M.; Li, Y.; Sukari, A.; Ou, S. H. I.; Al-Hallak, M. N.; Azmi, A. S. KRAS G12C Game of Thrones, which Direct KRAS Inhibitor will Claim the Iron Throne? *Cancer Treat. Rev.* **2020**, *84*, 101974.
(20) Ostrem, J. M.; Peters, U.; Sos, M. L.; Wells, J. A.; Shokat, K. M. K-Ras(G12C) Inhibitors Allosterically Control GTP Affinity and Effector Interactions. *Nature* **2013**, *503* (7477), 548−551.
(21) Lito, P.; Solomon, M.; Li, L. S.; Hansen, R.; Rosen, N. Allele-Specific Inhibitors Inactivate Mutant KRAS G12C by a Trapping Mechanism. *Science* **2016**, *351* (6273), 604−608.
(22) Zhang, Z.; Morstein, J.; Ecker, A. K.; Guiley, K. Z.; Shokat, K. M. Chemoselective Covalent Modification of K-Ras(G12R) with a Small Molecule Electrophile. *J. Am. Chem. Soc.* **2022**, *144* (35), 15916−15921.
(23) Sharma, A. K.; Pei, J.; Yang, Y.; Dyba, M.; Smith, B.; Rabara, D.; Larsen, E. K.; Lightstone, F. C.; Esposito, D.; Stephen, A. G.; et al. Revealing the Mechanism of Action of a First-in-Class Covalent Inhibitor of KRASG12C (ON) and Other Functional Properties of Oncogenic KRAS by ^{31}P NMR. *J. Biol. Chem.* **2024**, *300* (2), 105650.
(24) Zheng, Q.; Zhang, Z.; Guiley, K. Z.; Shokat, K. M. Strain-Release Alkylation of Asp12 Enables Mutant Selective Targeting of K-Ras-G12D. *Nat. Chem. Biol.* **2024**, *20*, 1114−1122.
(25) Tomazini, A.; Shifman, J. M. Targeting Ras with Protein Engineering. *Oncotarget* **2023**, *14*, 672−687.
(26) Sogabe, S.; Kamada, Y.; Miwa, M.; Niida, A.; Sameshima, T.; Kamaura, M.; Yonemori, K.; Sasaki, S.; Sakamoto, J. i.; Sakamoto, K. Crystal Structure of a Human K-Ras G12D Mutant in Complex with GDP and the Cyclic Inhibitory Peptide KRpep-2d. *ACS Med. Chem. Lett.* **2017**, *8* (7), 732−736.
(27) Zhang, Z.; Gao, R.; Hu, Q.; Peacock, H.; Peacock, D. M.; Dai, S.; Shokat, K. M.; Suga, H. GTP-State-Selective Cyclic Peptide Ligands of K-Ras(G12D) Block Its Interaction with Raf. *ACS Cent. Sci.* **2020**, *6* (10), 1753−1761.
(28) Sakamoto, K.; Masutani, T.; Hirokawa, T. Generation of KS-58 as the First K-Ras(G12D)-Inhibitory Peptide Presenting Anti-Cancer Activity in vivo. *Sci. Rep.* **2020**, *10* (1), 21671.
(29) Lim, S.; Boyer, N.; Boo, N.; Huang, C.; Venkatachalam, G.; Angela Juang, Y. C.; Garrigou, M.; Kaan, H. Y. K.; Duggal, R.; Peh, K. M.; et al. Discovery of Cell Active Macrocyclic Peptides with On-Target Inhibition of KRAS Signaling. *Chem. Sci.* **2021**, *12* (48), 15975−15987.
(30) Pantsar, T. The Current Understanding of KRAS Protein Structure and Dynamics. *Comput. Struct. Biotechnol. J.* **2020**, *18*, 189−198.
(31) Ostrem, J. M. L.; Shokat, K. M. Direct Small-Molecule Inhibitors of KRAS: From Structural Insights to Mechanism-Based Design. *Nat. Rev. Drug Discovery* **2016**, *15* (11), 771−785.
(32) Patricelli, M. P.; Janes, M. R.; Li, L.; Hansen, R.; Peters, U.; Kessler, L. V.; Chen, Y.; Kucharski, J. M.; Feng, J.; Ely, T.; et al. Selective Inhibition of Oncogenic KRAS Output with Small Molecules Targeting the Inactive State. *Cancer Discov.* **2016**, *6* (3), 316−329.
(33) Janes, M. R.; Zhang, J.; Li, L.; Hansen, R.; Peters, U.; Guo, X.; Chen, Y.; Babbar, A.; Firdaus, S. J.; Darjania, L.; et al. Targeting KRAS Mutant Cancers with a Covalent G12C-Specific Inhibitor. *Cell* **2018**, *172* (3), 578−589.e17.
(34) Drosten, M.; Barbacid, M. KRAS Inhibitors: Going Non-covalent. *Mol. Oncol.* **2022**, *16* (22), 3911−3915.
(35) Kwan, A. K.; Piazza, G. A.; Keeton, A. B.; Leite, C. A. The Path to the Clinic: A Comprehensive Review on Direct KRAS^{G12C} Inhibitors. *J. Exp. Clin. Cancer Res.* **2022**, *41* (1), 27.
(36) Ning, W.; Yang, Z.; Kocher, G. J.; Dorn, P.; Peng, R. W. A Breakthrough Brought about by Targeting KRAS^{G12C}: Nonconformity Is Punished. *Cancers (Basel)* **2022**, *14* (2), 390.
(37) Awad, M. M.; Liu, S.; Rybkin, I. I.; Arbour, K. C.; Dilly, J.; Zhu, V. W.; Johnson, M. L.; Heist, R. S.; Patil, T.; Riely, G. J.; et al. Acquired Resistance to KRAS G12C Inhibition in Cancer. *N. Engl. J. Med.* **2021**, *384* (25), 2382−2393.
(38) Tanaka, N.; Lin, J. J.; Li, C.; Ryan, M. B.; Zhang, J.; Kiedrowski, L. A.; Michel, A. G.; Syed, M. U.; Fella, K. A.; Sakhi, M.; et al. Clinical Acquired Resistance to KRASG12C Inhibition through a Novel KRAS Switch-II Pocket Mutation and Polyclonal Alterations Converging on RAS−MAPK Reactivation. *Cancer Discov.* **2021**, *11* (8), 1913−1922.
(39) Ryan, M. B.; Coker, O.; Sorokin, A.; Fella, K.; Barnes, H.; Wong, E.; Kanikarla, P.; Gao, F.; Zhang, Y.; Zhou, L.; et al. KRAS^{G12C}-Independent Feedback Activation of Wild-Type RAS Constrains KRAS G12C Inhibitor Efficacy. *Cell Rep.* **2022**, *39* (12), 110993.
(40) Feng, S.; Callow, M. G.; Fortin, J.; Khan, Z.; Bray, D.; Costa, M.; Shi, Z.; Wang, W.; Evangelista, M. A Saturation Mutagenesis Screen Uncovers Resistant and Sensitizing Secondary KRAS Mutations to Clinical KRAS^{G12C} Inhibitors. *Proc. Natl. Acad. Sci. U.S.A.* **2022**, *119* (18), No. e2120512119.
(41) Jiao, D.; Yang, S. Overcoming Resistance to Drugs Targeting KRAS Mutation. *Innovation (Camb)* **2020**, *1* (2), 100035.
(42) Addeo, A.; Banna, G. L.; Friedlaender, A. KRAS G12C Mutations in NSCLC: From Target to Resistance. *Cancers (Basel)* **2021**, *13* (11), 2541.
(43) Liu, J.; Kang, R.; Tang, D. The KRAS-G12C Inhibitor: Activity and Resistance. *Cancer Gene Ther.* **2022**, *29* (7), 875−878.
(44) Koga, T.; Suda, K.; Fujino, T.; Ohara, S.; Hamada, A.; Nishino, M.; Chiba, M.; Shimoji, M.; Takemoto, T.; Arita, T.; et al. KRAS Secondary Mutations That Confer Acquired Resistance to KRAS G12C Inhibitors, Sotorasib and Adagrasib, and Overcoming Strategies: Insights From In Vitro Experiments. *J. Thorac. Oncol.* **2021**, *16* (8), 1321−1332.
(45) Di Federico, A.; Ricciotti, I.; Favorito, V.; Michelina, S. V.; Scaparone, P.; Metro, G.; De Giglio, A.; Pecci, F.; Lamberti, G.; Ambrogio, C.; et al. Resistance to KRAS G12C Inhibition in Non-small Cell Lung Cancer. *Curr. Oncol. Rep.* **2023**, *25* (9), 1017−1029.
(46) Singhal, A.; Li, B. T.; O'Reilly, E. M. Targeting KRAS in Cancer. *Nat. Med.* **2024**, *30* (4), 969−983.
(47) Wei, D.; Wang, L.; Zuo, X.; Maitra, A.; Bresalier, R. S. A Small Molecule with Big Impact: MRTX1133 Targets the KRASG12D Mutation in Pancreatic Cancer. *Clin. Cancer Res.* **2024**, *30* (4), 655−662.
(48) Hallin, J.; Bowcut, V.; Calinisan, A.; Briere, D. M.; Hargis, L.; Engstrom, L. D.; Laguer, J.; Medwid, J.; Vanderpool, D.; Lifset, E.; et al. Anti-tumor efficacy of a potent and selective non-covalent KRAS^{G12D} inhibitor. *Nat. Med.* **2022**, *28* (10), 2171−2182.
(49) Kopra, K.; Valtonen, S.; Mahran, R.; Kapp, J. N.; Hassan, N.; Gillette, W.; Dennis, B.; Li, L.; Westover, K. D.; Plückthun, A.; et al. Thermal Shift Assay for Small GTPase Stability Screening: Evaluation and Suitability. *Int. J. Mol. Sci.* **2022**, *23* (13), 7095.
(50) Vuorinen, E.; Valtonen, S.; Eskonen, V.; Kariniemi, T.; Jakovleva, J.; Kopra, K.; Härmä, H. Sensitive Label-Free Thermal Stability Assay for Protein Denaturation and Protein-Ligand Interaction Studies. *Anal. Chem.* **2020**, *92* (5), 3512−3516.
(51) Valtonen, S.; Vuorinen, E.; Kariniemi, T.; Eskonen, V.; Le Quesne, J.; Bushell, M.; Härmä, H.; Kopra, K. Nanomolar Protein−Protein Interaction Monitoring with a Label-Free Protein-Probe Technique. *Anal. Chem.* **2020**, *92* (24), 15781−15788.
(52) Kopra, K.; Vuorinen, E.; Abreu-Blanco, M.; Wang, Q.; Eskonen, V.; Gillette, W.; Pulliainen, A. T.; Holderfield, M.; Härmä, H. Homogeneous Dual-Parametric-Coupled Assay for Simultaneous Nucleotide Exchange and KRAS/RAF-RBD Interaction Monitoring. *Anal. Chem.* **2020**, *92* (7), 4971−4979.
(53) Kopra, K.; Ligabue, A.; Wang, Q.; Syrjänpää, M.; Blaževitš, O.; Veltel, S.; van Adrichem, A. J.; Hänninen, P.; Abankwa, D.; Härmä, H. A Homogeneous Quenching Resonance Energy Transfer Assay for the Kinetic Analysis of the GTPase Nucleotide Exchange Reaction. *Anal. Bioanal. Chem.* **2014**, *406* (17), 4147−4156.

https://doi.org/10.1021/acschembio.4c00315
ACS Chem. Biol. XXXX, XXX, XXX−XXX

(54) Kopra, K.; van Adrichem, A. J.; Salo-Ahen, O. M. H.; Peltonen, J.; Wennerberg, K.; Härmä, H. High-Throughput Dual Screening Method for Ras Activities and Inhibitors. *Anal. Chem.* **2017**, *89* (8), 4508−4516.
(55) Kopra, K.; Härmä, H. Methods to Monitor Ras Activation State. In *Ras Activity and Signaling*; Rubio, I., Prior, I., Eds.; *Methods Mol. Biol.*, 2021; Vol. *2262*, pp 137−167.
(56) Lanman, B. A.; Allen, J. R.; Allen, J. G.; Amegadzie, A. K.; Ashton, K. S.; Booker, S. K.; Chen, J. J.; Chen, N.; Frohn, M. J.; Goodman, G.; et al. Discovery of a Covalent Inhibitor of KRASG12C (AMG 510) for the Treatment of Solid Tumors. *J. Med. Chem.* **2020**, *63* (1), 52−65.
(57) Fell, J. B.; Fischer, J. P.; Baer, B. R.; Blake, J. F.; Bouhana, K.; Briere, D. M.; Brown, K. D.; Burgess, L. E.; Burns, A. C.; Burkard, M. R.; et al. Identification of the Clinical Development Candidate MRTX849, a Covalent $KRAS^{G12C}$ Inhibitor for the Treatment of Cancer. *J. Med. Chem.* **2020**, *63* (13), 6679−6693.
(58) Canon, J.; Rex, K.; Saiki, A. Y.; Mohr, C.; Cooke, K.; Bagal, D.; Gaida, K.; Holt, T.; Knutson, C. G.; Koppada, N.; et al. The Clinical KRAS(G12C) Inhibitor AMG 510 Drives Anti-Tumour Immunity. *Nature* **2019**, *575* (7781), 217−223.
(59) Mortison, J. D.; Cornella-Taracido, I.; Venkatchalam, G.; Partridge, A. W.; Siriwardana, N.; Bushell, S. M. Rapid Evaluation of Small Molecule Cellular Target Engagement with a Luminescent Thermal Shift Assay. *ACS Med. Chem. Lett.* **2021**, *12* (8), 1288−1294.
(60) Valtonen, S.; Vuorinen, E.; Eskonen, V.; Malakoutikhah, M.; Kopra, K.; Härmä, H. Sensitive, homogeneous, and label-free protein-probe assay for antibody aggregation and thermal stability studies. *MAbs* **2021**, *13* (1), 1955810.
(61) Hallin, J.; Engstrom, L. D.; Hargis, L.; Calinisan, A.; Aranda, R.; Briere, D. M.; Sudhakar, N.; Bowcut, V.; Baer, B. R.; Ballard, J. A.; et al. The $KRAS^{G12C}$ Inhibitor MRTX849 Provides Insight Toward Therapeutic Susceptibility of KRAS-Mutant Cancers in Mouse Models and Patients. *Cancer Discov.* **2020**, *10* (1), 54−71.
(62) Kopra, K. Luminescence-Based Techniques for KRAS Thermal Stability Monitoring. In *KRAS*; Stephen, A. G., Esposito, D., Eds.; *Methods Mol. Biol.*, 2024; Vol. *2797*, pp 125−143.
(63) Alexander, P.; Stephen, A. Affinity Measurement of Non-covalent Interactions of the Covalent KRAS G12C GDP Inhibitor MRTX849 to RAS Isoforms Using Surface Plasmon Resonance. In *KRAS*; Stephen, A. G., Esposito, D., Eds.; *Methods Mol. Biol.*, 2024; Vol. *2797*, pp 103−113.
(64) Food and Drug Administration (FDA), Center for Drug Evaluation and Research (CBER). *NDA/BLA Multi-Disciplinary Review and Evaluation {NDA 216340}{KRAZATI (Adagrasib)}, Application Number: 216340Orig1s000: USA*, 2021. https://www.accessdata.fda.gov/drugsatfda_docs/nda/2023/216340Orig1s000MultidisciplineR.pdf (accessed 07 01, 2024).
(65) Rubinson, D. A.; Tanaka, N.; de la Cruz, F. F.; et al. Sotorasib is a Pan-RASG12C Inhibitor Capable of Driving Clinical Response in NRASG12C Cancers. *Cancer Discov.* **2024**, *14*, 727.
(66) Tate, J. G.; Bamford, S.; Jubb, H. C.; Sondka, Z.; Beare, D. M.; Bindal, N.; Boutselakis, H.; Cole, C. G.; Creatore, C.; Dawson, E.; et al. COSMIC: the Catalogue of Somatic Mutations in Cancer. *Nucleic Acids Res.* **2019**, *47* (D1), D941−D947.
(67) Boriack-Sjodin, P. A.; Margarit, S. M.; Bar-Sagi, D.; Kuriyan, J. The Structural Basis of the Activation of Ras by Sos. *Nature* **1998**, *394* (6691), 337−343.
(68) Hillig, R. C.; Sautier, B.; Schroeder, J.; Moosmayer, D.; Hilpmann, A.; Stegmann, C. M.; Werbeck, N. D.; Briem, H.; Boemer, U.; Weiske, J.; et al. Discovery of Potent SOS1 Inhibitors that Block RAS Activation via Disruption of the RAS−SOS1 Interaction. *Proc. Natl. Acad. Sci. U.S.A.* **2019**, *116* (7), 2551−2560.
(69) Wang, X.; Allen, S.; Blake, J. F.; Bowcut, V.; Briere, D. M.; Calinisan, A.; Dahlke, J. R.; Fell, J. B.; Fischer, J. P.; Gunn, R. J.; et al. Identification of MRTX1133, a Noncovalent, Potent, and Selective KRASG12D Inhibitor. *J. Med. Chem.* **2022**, *65* (4), 3123−3133.
(70) Nilewski, C.; Labadie, S.; Wei, B.; Malhotra, S.; Do, S.; Gazzard, L.; Liu, L.; Shao, C.; Murray, J.; Izrayelit, Y.; et al. Structure-Based Design and Evaluation of Reversible KRAS G13D Inhibitors. *ACS Med. Chem. Lett.* **2024**, *15* (1), 21−28.
(71) Burd, C. E.; Liu, W.; Huynh, M. V.; Waqas, M. A.; Gillahan, J. E.; Clark, K. S.; Fu, K.; Martin, B. L.; Jeck, W. R.; Souroullas, G. P.; et al. Mutation-Specific RAS Oncogenicity Explains NRAS Codon 61 Selection in Melanoma. *Cancer Discov.* **2014**, *4* (12), 1418−1429.
(72) Muñoz-Maldonado, C.; Zimmer, Y.; Medová, M. A Comparative Analysis of Individual RAS Mutations in Cancer Biology. *Front. Oncol.* **2019**, *9*, 1088.
(73) Lim, S.; Khoo, R.; Juang, Y.-C.; Gopal, P.; Zhang, H.; Yeo, C.; Peh, K. M.; Teo, J.; Ng, S.; Henry, B.; et al. Exquisitely Specific anti-KRAS Biodegraders Inform on the Cellular Prevalence of Nucleotide-Loaded States. *ACS Cent. Sci.* **2021**, *7* (2), 274−291.
(74) Huynh, M. V.; Hobbs, G. A.; Schaefer, A.; Pierobon, M.; Carey, L. M.; Diehl, J. N.; DeLiberty, J. M.; Thurman, R. D.; Cooke, A. R.; Goodwin, C. M.; et al. Functional and Biological Heterogeneity of $KRAS^{Q61}$ Mutations. *Sci. Signal* **2022**, *15* (746), No. eabn2694.
(75) Li, J.; Zhao, J.; Cao, B.; Fang, J.; Li, X.; Wang, M.; Ba, Y.; Li, X.; Li, Z.; Liu, Z.; et al. A Phase I/II Study of First-in-Human Trial of JAB-21822 (KRAS G12C Inhibitor) in Advanced Solid Tumors. *J. Clin. Oncol.* **2022**, *40*, 3089.
(76) Li, Z.; Song, Z.; Zhao, Y.; Wang, P.; Jiang, L.; Gong, Y.; Zhou, J.; Jian, H.; Dong, X.; Zhuang, W.; et al. D-1553 (Garsorasib), a Potent and Selective Inhibitor of KRASG12C in Patients with NSCLC: Phase 1 Study Results. *J. Thorac. Oncol.* **2023**, *18* (7), 940−951.
(77) Ma, X.; Sloman, D. L.; Duggal, R.; Anderson, K. D.; Ballard, J. E.; Bharathan, I.; Brynczka, C.; Gathiaka, S.; Henderson, T. J.; Lyons, T. W.; et al. Discovery of MK-1084: An Orally Bioavailable and Low-Dose KRASG12C Inhibitor. *J. Med. Chem.* **2024**, *67*, 11024−11052.
(78) Blaquier, J. B.; Cardona, A. F.; Recondo, G. Resistance to $KRAS^{G12C}$ Inhibitors in Non-Small Cell Lung Cancer. *Front. Oncol.* **2021**, *11*, 787585.
(79) Syrjänpää, M.; Vuorinen, E.; Kulmala, S.; Wang, Q.; Härmä, H.; Kopra, K. QTR-FRET: Efficient Background Reduction Technology in Time-resolved Förster Resonance Energy Transfer Assays. *Anal. Chim. Acta* **2019**, *1092*, 93−101.
(80) Vuorinen, E.; Valtonen, S.; Hassan, N.; Mahran, R.; Habib, H.; Malakoutikhah, M.; Kopra, K.; Härmä, H. Protease Substrate-Independent Universal Assay for Monitoring Digestion of Native Unmodified Proteins. *Int. J. Mol. Sci.* **2021**, *22* (12), 6362.
(81) Harder, E.; Damm, W.; Maple, J.; Wu, C.; Reboul, M.; Xiang, J. Y.; Wang, L.; Lupyan, D.; Dahlgren, M. K.; Knight, J. L.; et al. OPLS3: A Force Field Providing Broad Coverage of Drug-like Small Molecules and Proteins. *J. Chem. Theory Comput.* **2016**, *12* (1), 281−296.
(82) Roos, K.; Wu, C.; Damm, W.; Reboul, M.; Stevenson, J. M.; Lu, C.; Dahlgren, M. K.; Mondal, S.; Chen, W.; Wang, L.; et al. OPLS3e: Extending Force Field Coverage for Drug-Like Small Molecules. *J. Chem. Theory Comput.* **2019**, *15* (3), 1863−1874.
(83) Bowers, K. J.; Chow, D. E.; Xu, H.; et al. Scalable Algorithms for Molecular Dynamics Simulations on Commodity Clusters. *SC '06: Proceedings of the 2006 ACM/IEEE Conference on Supercomputing, Tampa, Florida, USA, Nov 11−17, 2006*; ACM Press: New York, USA, 2006; p 84.
(84) Madhavi Sastry, G.; Adzhigirey, M.; Day, T.; Annabhimoju, R.; Sherman, W. Protein and Ligand Preparation: Parameters, Protocols, and Influence on Virtual Screening Enrichments. *J. Comput. Aided Mol. Des.* **2013**, *27* (3), 221−234.
(85) Jorgensen, W. L.; Chandrasekhar, J.; Madura, J. D.; Impey, R. W.; Klein, M. L. Comparison of Simple Potential Functions for Simulating Liquid Water. *J. Chem. Phys.* **1983**, *79*, 926−935.
(86) Pantsar, T.; Kaiser, P. D.; Kudolo, M.; Forster, M.; Rothbauer, U.; Laufer, S. A. Decisive Role of Water and Protein Dynamics in Residence Time of p38α MAP Kinase Inhibitors. *Nat. Commun.* **2022**, *13* (1), 569.

https://doi.org/10.1021/acschembio.4c00315
ACS Chem. Biol. XXXX, XXX, XXX−XXX